Aerospace Science and Technology 145 (2024) 108904

Contents lists available at ScienceDirect

Aerospace Science and Technology

journal homepage: www.elsevier.com/locate/aescte

The effect of a nonlinear energy sink on the gust response of a wing

M.R. Amoozgar [a,*], A. Castrichini [b], S.D. Garvey [a], M.I. Friswell [c], J.E. Cooper [d], R.M. Ajaj [e]

[a] Faculty of Engineering, University of Nottingham, Nottingham NG7 2RD, United Kingdom
[b] Airbus Operations Ltd, Bristol, BS34 7QQ, United Kingdom
[c] Faculty of Science and Engineering, Swansea University, SA1 8EN, Swansea, United Kingdom
[d] Department of Aerospace Engineering, University of Bristol, Bristol, United Kingdom
[e] Advanced Research and Innovation Center (ARIC), Department of Aerospace Engineering, Khalifa University of Science and Technology, Abu Dhabi, 12778, United Arab Emirates

ARTICLE INFO

Communicated by Grigorios Dimitriadis

ABSTRACT

In this paper, the potential effectiveness of a nonlinear energy sink (NES) to absorb the energy from a wing that is vibrating as a result of flying in a gusty environment is investigated. The structural dynamics of the wing is simulated using a rigid airfoil mounted on two linear/nonlinear springs to represent the bending and torsional stiffness of the wing. The wing is subjected to a combination of gust and aerodynamic loads. The unsteady aerodynamic lift and moment are modelled using Wagner's theory. Furthermore, the gust loads are obtained by assuming two different gust profiles, e.g. sharp-edged and 1-cosine gust profiles. A nonlinear energy sink, which comprises of a concentrated mass, damper and a nonlinear spring, is attached to the wing, and its effectiveness to absorb the gust energy is investigated. The coupled nonlinear aeroelastic equations are integrated numerically to determine the response of the wing. To verify the developed aeroelastic model, the obtained results are compared with the available results in the literature and an excellent agreement is observed. The results highlight that adding the NES to the wing is capable of reducing the gust oscillation amplitude of the wing significantly when the NES parameters are chosen accordingly.

1. Introduction

Aeroelasticity is the interaction between elastic, inertia and aerodynamics forces [1,2]. The interaction between these forces can cause the aircraft to lose its stability (flutter). Therefore, understanding the aeroelastic behaviour of flying vehicles is crucial as the aircraft needs to remain inside the stability region for the whole service flight envelope. Using linear theories to simulate the aeroelastic behaviour of aircraft can generally give accurate predictions of the onset of the stability, and have been used for many years. However, in some occasions when nonlinearities are dominant in the system, these linear theories fail to draw a complete picture of the aeroelastic behaviour of the aircraft. For instance, when the aircraft flies at high angle of attack, high subsonic or transonic flight conditions etc., the aerodynamic nonlinearities become significant [3]. Furthermore, the structural nonlinearities such as loose control linkages, material nonlinearities, large deformation or worn hinges can also affect the aeroelasticity of the aircraft [4]. The structural nonlinearities can be categorised into distributed and concentrated nonlinearities [3].

When a thin wing twist angle increases due to the applied loads, the wing becomes stiffer and hence it will most likely behave like a hardening spring. In most of the previous studies, a cubic nonlinearity has been used to replicate this nonlinear stiffness behaviour of the wing [5–7]. One of the first studies dealing with the flutter analysis of aircraft wings with structural nonlinearities was considered by Woolston et al. [8]. The structural nonlinearity was modelled by using a concentrated nonlinear torsional stiffness, and it was shown that it has significant effects on both pre and post instability of the wing. Lee et al. [9] investigated the flutter of a typical section with free-play nonlinearity. They highlighted that depending on the system parameters, the wing can experience damped, limited amplitude or divergent oscillations. Several other studies also considered the effects of various structural nonlinearities on the aeroelasticity of wings [9–13]. Generally speaking, a two degree of freedom airfoil with nonlinearity in the pitch degree of freedom may experience a complex aeroelastic behaviour. For example, the system might experience a period-1, period-2, or period-4 limit cycle oscillations or a chaotic motion, depending on the flow velocity and system parameters [3].

* Corresponding author.
E-mail address: m.amoozgar@nottingham.ac.uk (M.R. Amoozgar).

https://doi.org/10.1016/j.ast.2024.108904
Received 18 May 2023; Received in revised form 10 January 2024; Accepted 17 January 2024
Available online 22 January 2024

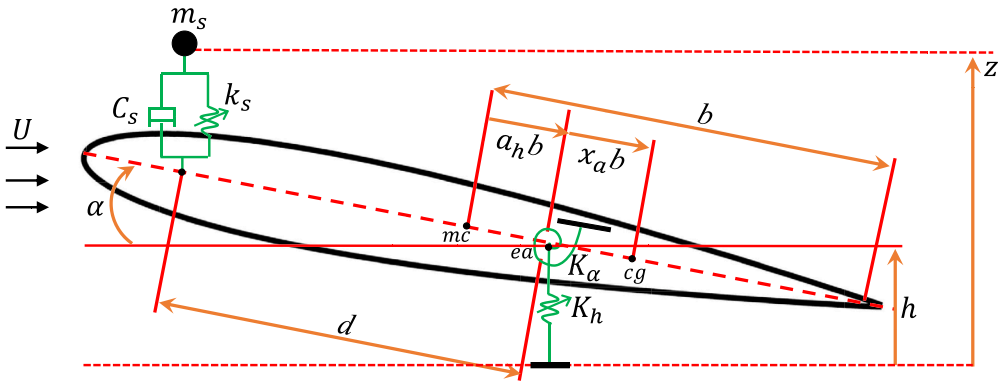

Fig. 1. Schematic of the 2D wing with NES.

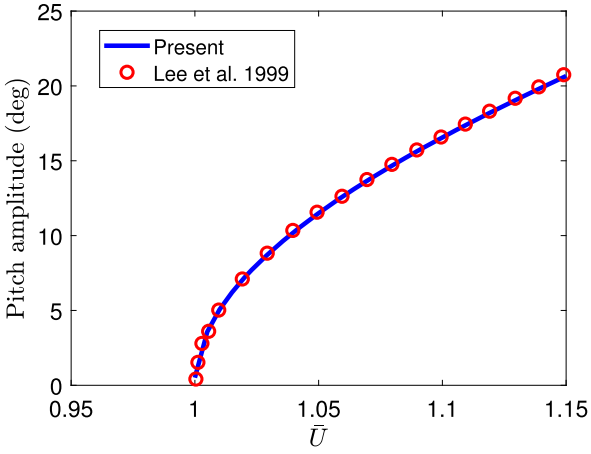

Fig. 2. Wing pitch amplitude for $\bar{\omega} = 0.2, \mu = 100, a_h = -0.5, x_\alpha = 0.25, r_\alpha = 0.5, \beta_0 = 1, \beta_\alpha = 3$.

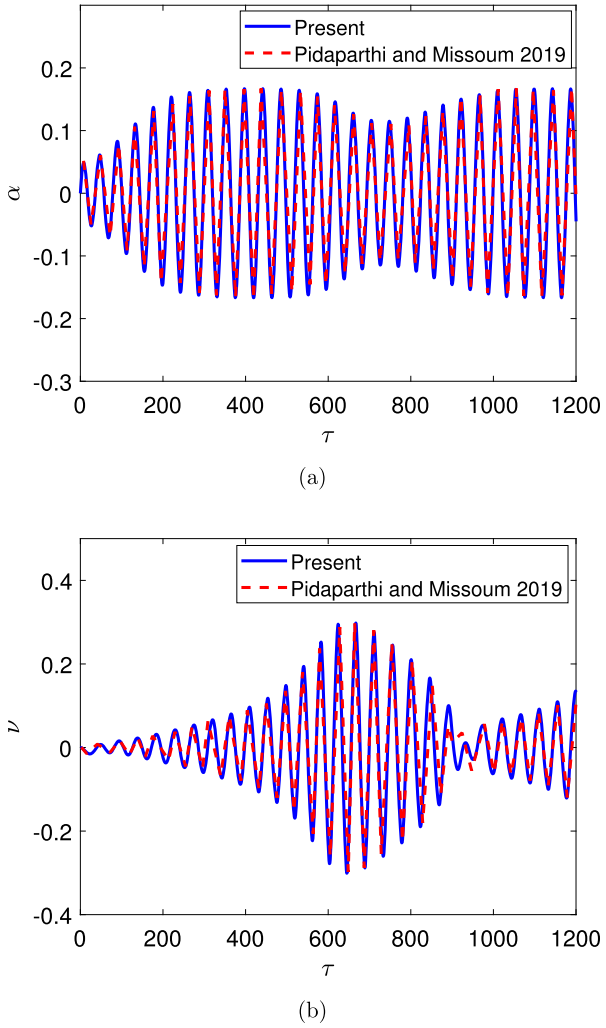

Fig. 3. The a) pitch and b) NES response for $\bar{U}/\bar{U}_f = 1.05, \bar{\omega} = 0.5, \mu = 100, a_h = -0.5, x_\alpha = 0.25, r_\alpha = 0.5, \beta_0 = 1, \beta_\alpha = 3, \gamma_\alpha = 20, C = 10, \lambda = 0.2, \epsilon = 0.01, \delta = 0.45$.

In linear systems, when the aircraft speed is lower than the aeroelastic instability speed, the dynamic response of the wing is damped. However, when the speed goes beyond this critical velocity, in reality the system might experience limit cycle oscillations (LCO), due to nonlinearities [14]. Based on the current design requirements, the aircraft should not enter into this unstable region and indeed avoid it with by a safety margin which limits the operational speeds. However, it may be possible to mitigate such unwanted oscillations actively or passively, and extend the flight envelope of the aircraft. A nonlinear energy sink (NES) device can be used as a way to reduce the limit cycle oscillation of wings passively [15,14]. This concept has been used to suppress the vibrations of various systems [15,16]. Generally speaking, a NES device is a mass-spring-damper system which is characterised by a nonlinear spring. Unlike a classical tuned-mass-damper, a properly designed NES is able to rapidly localize and dissipate the external dynamic energy over a wide range of frequencies [17]. The NES is capable of transferring the vibratory energy from the host/main system to the NES, hence reduce the vibration level of the host system. Bichiou et al. [15] showed that depending on the NES mass and location, it can be effective to change a subcritical bifurcation to a supercritical bifurcation. Due to the nonlinear nature of a NES, it can interact with various modes of the host structure, and this has been clarified by Jiang et al. [18] using both numerical and experimental methods. Malatkar and Nayfeh [19] showed that the mass of the NES directly affects the vibration amplitude reduction of a lightly damped subsystem. The concept of the NES has also been used for mitigation of the aeroelastic response of a 3D wing in hypersonic flow [20]. Their results revealed that the NES has stabilizing effects on the system. Zhou et al. [21] studied the effect of a nonlinear energy sink on the suppression of panel flutter response of a wing flying in supersonic flow. It was concluded that the device can suppress the response amplitude only when the transient energy of the NES and panel are comparable. More recently, Pidaparthi and Missoum [14] developed an optimised NES which is able to mitigate the

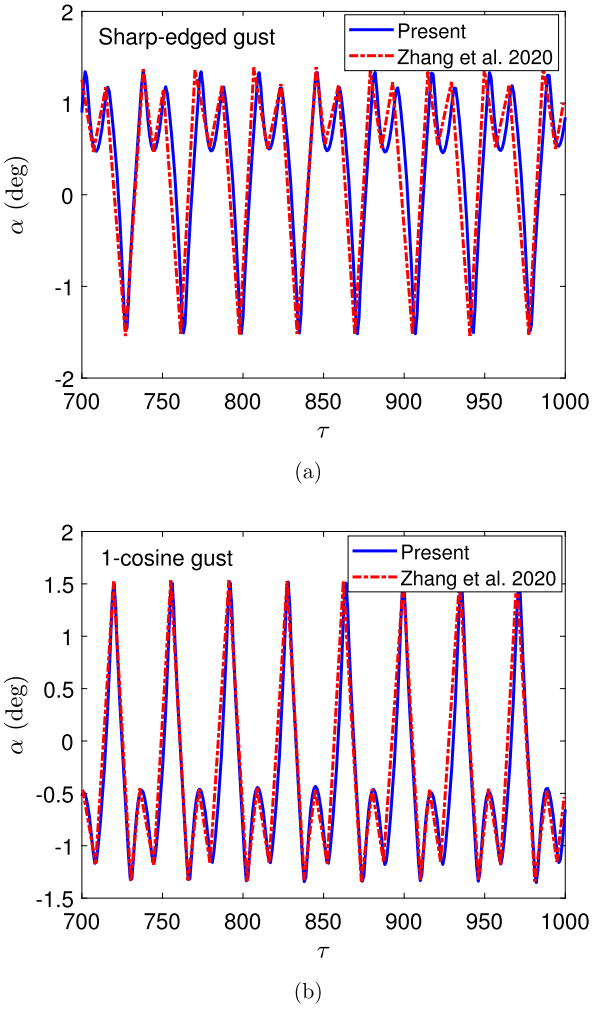

Fig. 4. The Pitch response of the wing subjected to a) sharp-edged gust and b) 1-cosine gust profiles for $\bar{U}/\bar{U}_f = 0.2$.

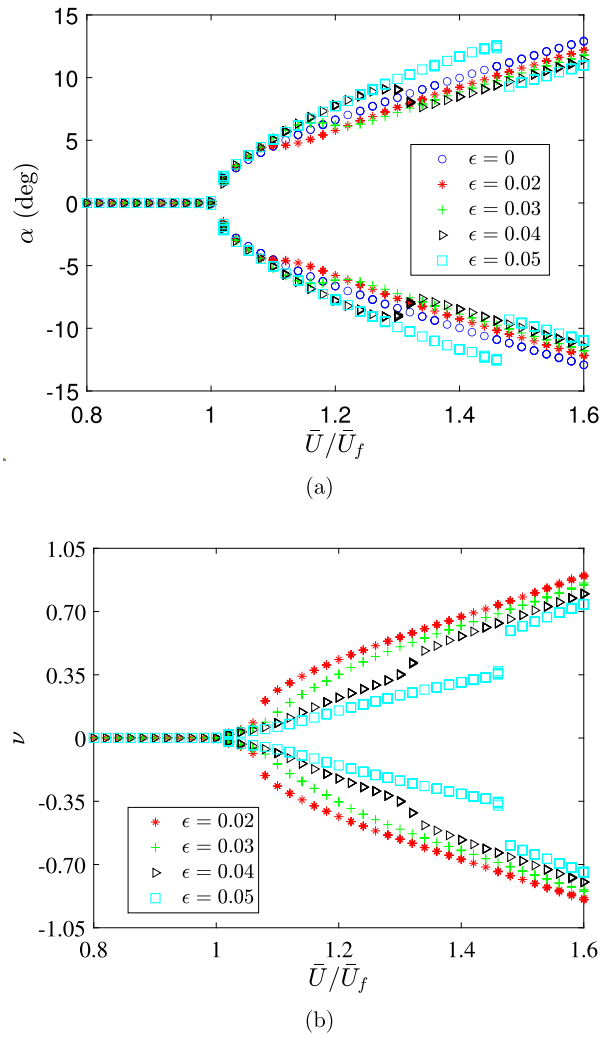

Fig. 5. The effect of NES mass ratio on bifurcation diagrams of case 1 wing for a) pitch and b) NES.

limit cycle oscillations of a nonlinear wing. They showed that if the NES parameters are designed accordingly for a system, it can reduce the vibration amplitude significantly.

An aircraft structure has to withstand all the loads applied to it during flight and ground manoeuvrers. One of the most extreme dynamic loads that the aircraft experiences during flight are the gust loads. Although the worst gust condition might happen rarely for the aircraft during its lifetime, the structure has to be designed to withstand these rare load cases [22,23]. Poirel and Price [24] studied the effect of longitudinal atmospheric turbulence on the dynamics of a wing with cubic nonlinearity. They showed that as the longitudinal gust acts via the airspeed, it has a parametric nature, and hence can affect the dynamic stability of the wing unlike the vertical and lateral gusts. Tang and Dowell [25] considered the gust response of a high aspect ratio wing numerically and experimentally using a nonlinear beam model combined with a dynamic stall aerodynamic model. Several other studies also considered the effect of gusts on the loads and response of wings [26–30]. While the current requirement is to design the structure to withstand all such loads applied to the wing, several studies investigated load alleviation concepts as a way to remove the structural design limitations and reduce the overall weight of the structure [31,32,22,33]. Castrichini et al. [31,34] studied the effect of a hinged wingtip to reduce larger load cases of the wing during flight. They showed that this device can reduce the dynamic loads of the wing. This concept was further investigated experimentally, and its effectiveness in various conditions was evaluated [35,36]. Passive gust loads alleviation using an inerter-based device for truss-braced wings was studied by Szczyglowski et al. [22]. They showed that a 4% gust load reduction can be achieved by using a combination of inerter-based devices. Khalil and Fezans [33] designed a combined feedback/feedforward controller for gust load alleviation system of a flexible aircraft. The proposed method was based on the H_∞-optimal control technique, and its effectiveness was shown. Courcy et al. [37] considered the effect of sloshing in wing fuel tanks as a means of increasing the structural damping to alleviate flight loads. The numerical and experimental results showed that the fuel sloshing can increase the structural damping and hence reduce the wing loads, but it is dependent upon the tank location, size and fill ratio. A model predictive control was developed by Wuestenhagen [38] as augmentation to an aircraft in gust conditions. The gust load alleviation control method estimates the bending moment at wing root, and controls the control surface deflection and rate in different mass and flight conditions.

Although the concept of NES has previously shown to be promising for limit cycle oscillation amplitude reduction of aircraft wings, its effectiveness on gust load attenuation has never been investigated. This paper reports an initial study of the effectiveness of nonlinear energy sinks on gust load reduction of aircraft wings. To this aim, first, the aeroelastic equations of a wing-NES system with hardening nonlinearities subjected to a gust are developed, and then verified. Finally, a parametric study is performed to evaluate the effect of NES parameters on the aeroelastic and gust response of the wing.

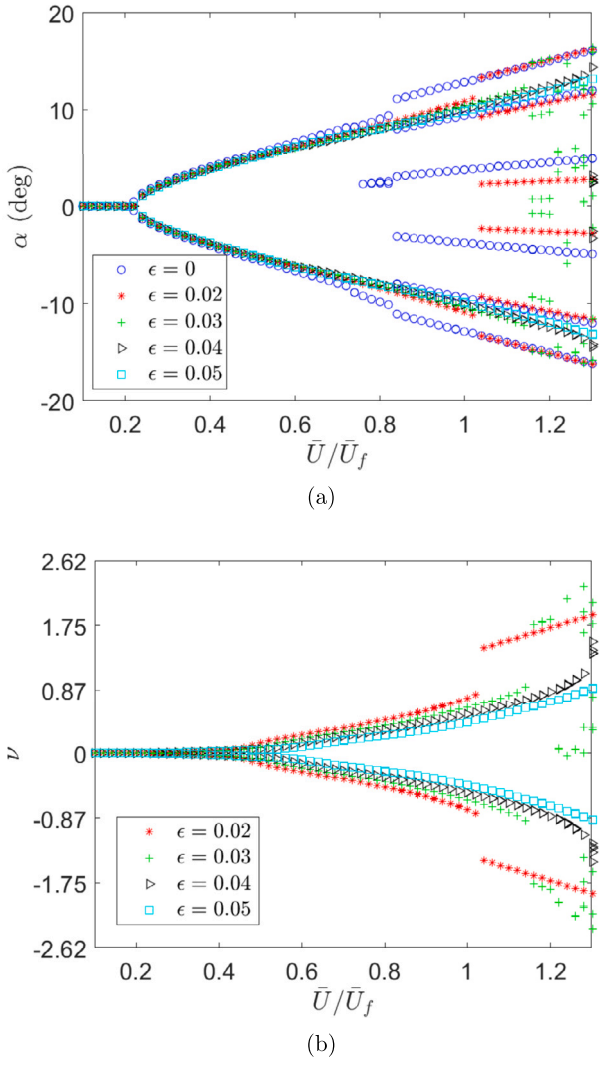

Fig. 6. The effect of NES mass ratio on bifurcation diagrams of case 2 wing for a) pitch and b) NE.

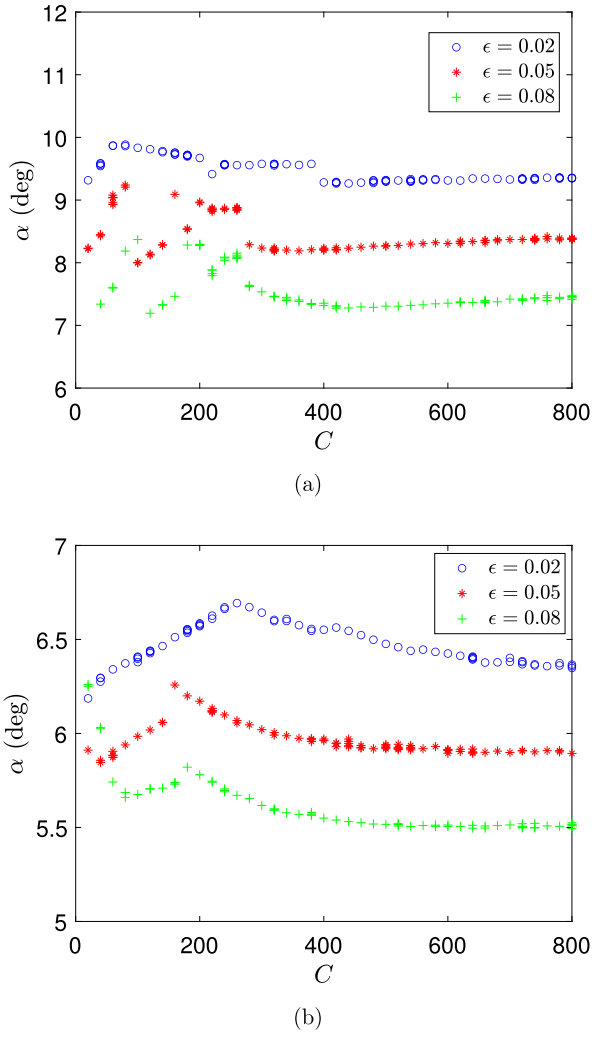

Fig. 7. The effect of NES stiffness on the pitch response of a) case 1 wing at $\bar{U}/\bar{U}_f = 1.4$ and b) case 2 wing at $\bar{U}/\bar{U}_f = 0.6$.

2. Problem description and modelling

A two degrees of freedom wing with a nonlinear energy sink, as shown in Fig. 1, is considered. The bending and torsional stiffness of the wing are simulated using two springs (k_h and k_α) which are attached to the elastic axis of the wing (e.a) [14]. Also, the total mass of the wing (m) is concentrated on the wing mass centre (cg). A nonlinear energy sink, which is composed of a mass (m_s), a linear damper (c_s) and a nonlinear spring (k_s), located at a distance of d from the wing elastic axis (ea) is considered. The wing is subjected to a combination of aerodynamic loads and gust loads, and the airflow velocity is denoted by U. The downward plunge deflection (h) and NES position (z), and nose up pitch deflection (α) are considered as positive directions. The aeroelastic equations of motion of this system can be written as [14]

$$m\ddot{h} + S_\alpha\ddot{\alpha} + c_h\dot{h} + \bar{G}(h) + c_s(\dot{h} - \dot{\alpha}d - \dot{z}) + k_s(h - \alpha d - z)^3 = Q_h \quad (1)$$

$$S_\alpha\ddot{h} + I_\alpha\ddot{\alpha} + c_\alpha\dot{\alpha} + \bar{M}(\alpha) + c_s d(\dot{\alpha}d + \dot{z} - \dot{h}) + k_s d(\alpha d + z - h)^3 = Q_\alpha \quad (2)$$

$$m_s\ddot{z} + c_s(\dot{z} + \dot{\alpha}d - \dot{h}) + k_s(z + \alpha d - h)^3 = 0 \quad (3)$$

where $\bar{G}(h)$ and $\bar{M}(\alpha)$ are the linear/nonlinear plunge and pitch stiffness terms, and S_α and I_α are first and second mass moment of inertia about the wing elastic axis. Also, m, c_h and c_α are wing's mass, plunge and pitch damping coefficients, respectively. Furthermore, the NES's mass, stiffness and damping are denoted by m_s, k_s and c_s. Q_h and Q_α are the total lift and moments on the airfoil which can be written as

$$\begin{aligned} Q_h &= L_a + L_g \\ Q_\alpha &= M_a + M_g \end{aligned} \quad (4)$$

where indices $()_a$ and $()_g$ refer to aerodynamic and gust loads, respectively. By defining the dimensionless parameters

$$\xi = h/b,\ \nu = z/b,\ \tau = Ut/b,\ \bar{U} = U/b\omega_\alpha,\ \bar{\omega} = \omega_\xi/\omega_\alpha,\ x_\alpha = S_\alpha/bm,$$

$$\omega_\xi = \sqrt{k_h/m},\ \omega_\alpha = \sqrt{k_\alpha/I_\alpha},\ \zeta_\xi = c_h/2\sqrt{mk_h},\ \zeta_\alpha = c_\alpha/2\sqrt{I_\alpha k_\alpha},$$

$$r_\alpha = \sqrt{I_\alpha/mb^2},\ \epsilon = m_s/m,\ C = k_s b^2/m_s\omega_\alpha^2,\ \lambda = c_s/m_s\omega_\alpha,$$

$$\delta = d/b,\ \mu = m/\pi\rho b^2$$

the coupled aeroelastic equations can be written in nondimensional form as

$$\xi'' + x_\alpha\alpha'' + 2\zeta_\xi\frac{\bar{\omega}}{\bar{U}}\xi' + (\frac{\bar{\omega}}{\bar{U}})^2 G(\xi) + \frac{\epsilon\lambda}{\bar{U}}(\xi' - \delta\alpha' - \nu') + \frac{\epsilon C}{\bar{U}^2}(\xi - \delta\alpha - \nu)^3 = l_a + l_g \quad (5)$$

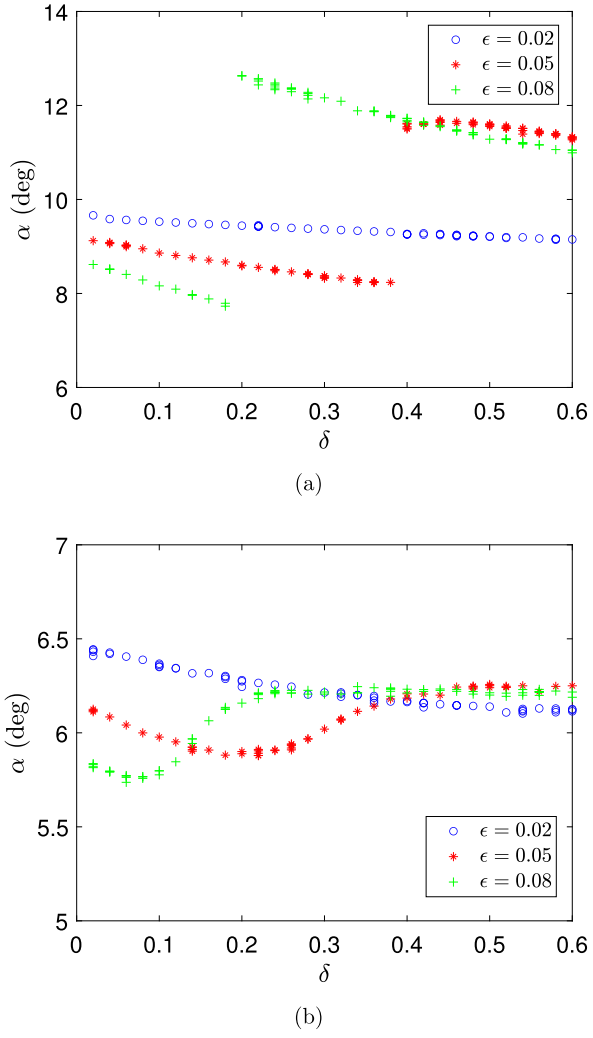

Fig. 8. The effect of NES location on the pitch response of a) case 1 wing at $\bar{U}/\bar{U}_f = 1.4$ and b) case 2 wing at $\bar{U}/\bar{U}_f = 0.6$.

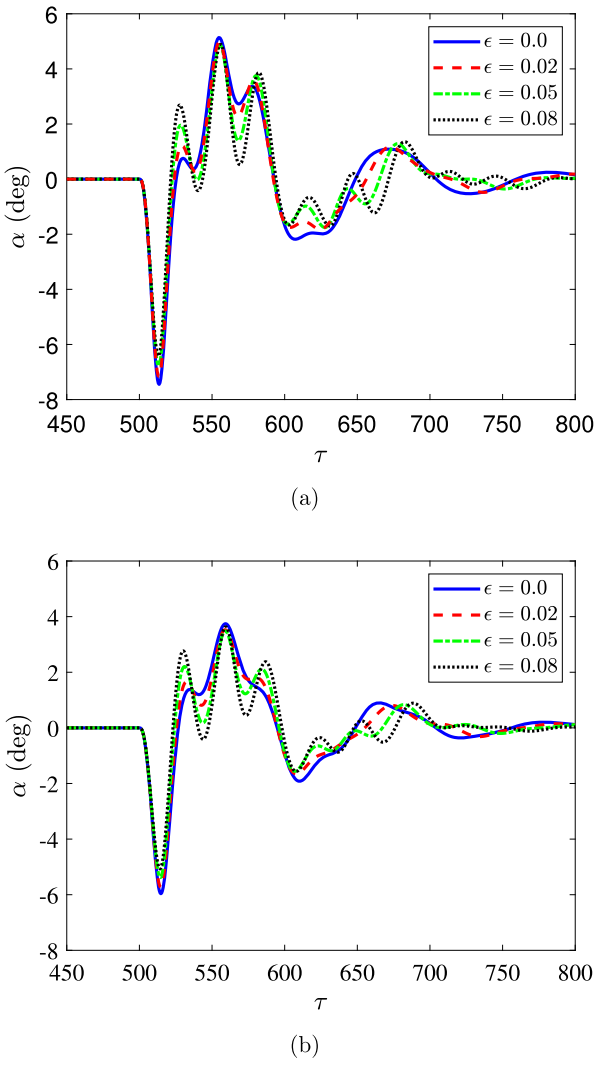

Fig. 9. The effect of NES mass ratio on the gust response of the wing for $w_0 = 0.2$ a) sharp-edged gust profile b) 1-cosine gust profile.

$$\frac{x_\alpha}{r_\alpha^2}\xi'' + \alpha'' + 2\frac{\zeta_\alpha}{\bar{U}}\alpha' + \frac{1}{\bar{U}^2}M(\alpha) + \frac{\delta\epsilon\lambda}{r_\alpha^2\bar{U}}(\delta\alpha' + \nu' - \xi') + \frac{\delta\epsilon C}{r_\alpha^2\bar{U}^2}(\delta\alpha + \nu - \xi)^3 = m_a + m_g \tag{6}$$

$$\nu'' + \frac{\lambda}{\bar{U}}(\nu' + \delta\alpha' - \xi') + \frac{C}{\bar{U}^2}(\nu + \delta\alpha - \xi)^3 = 0 \tag{7}$$

The unsteady aerodynamic lift and moment can be obtained as [39]

$$l_a = -\frac{1}{\mu}(\alpha' + \xi'' - a_h\alpha'') - \frac{2}{\mu}\int_0^\infty \phi(\tau-\sigma)(\alpha' + \xi'' + (0.5 - a_h)\alpha'')d\sigma \tag{8}$$

$$m_a = -\frac{a_h}{r_\alpha^2\mu}(\xi'' - a_h\alpha'') - \frac{1}{r_\alpha^2\mu}(0.5 - a_h)\alpha' - \frac{1}{8r_\alpha^2\mu}\alpha'' + \frac{2}{\mu}(0.5 + a_h)\int_0^\infty \phi(\tau-\sigma)(\alpha' + \xi'' + (0.5 - a_h)\alpha'')d\sigma \tag{9}$$

where a_h is the offset between elastic axis and mid-chord, and $\phi(\tau)$ is the Wagner function which can be approximated as [1]

$$\phi(\tau) = 1 - A_1 e^{-b_1\tau} - A_2 e^{-b_2\tau}, (\tau > 0) \tag{10}$$

where $A_1 = 0.165$, $A_2 = 0.335$, $b_1 = 0.0455$ and $b_2 = 0.3$. Furthermore, the gust lift and moment about the elastic axis can be obtained as [39]

$$l_g = \frac{2}{\mu}\int_0^\tau \psi'(\tau-\sigma)\bar{w_g}d\sigma \tag{11}$$

$$m_g = (0.5 + a_h)\frac{2}{r_\alpha^2\mu}\int_0^\tau \psi'(\tau-\sigma)\bar{w_g}d\sigma \tag{12}$$

where $\bar{w_g} = w_g/U$ is the nondimensional gust velocity, and $\psi(\tau)$ is the Küssner's function which can be defined as [3]

$$\psi(\tau) = 1 - A_3 e^{-b_3\tau} - A_4 e^{-b_4\tau} \tag{13}$$

where $A_3 = 0.5$, $A_4 = 0.5$, $b_3 = 0.13$ and $b_4 = 1$.

In this study, "sharp-edged" and "1-cosine" gust profiles are used which can be defined as [39]

$$\text{sharp-edged gust}: \quad \bar{w_g}(\tau) = H(\tau)\bar{w}_0 \tag{14}$$

$$\text{1-cosine gust}: \quad \bar{w_g}(\tau) = \frac{1}{2}H(\tau)\bar{w}_0(1 - \cos\frac{\pi\tau}{\tau_g}) - \frac{1}{2}H(\tau - 2\tau_g)\bar{w}_0(1 - \cos\frac{\pi\tau}{\tau_g}) \tag{15}$$

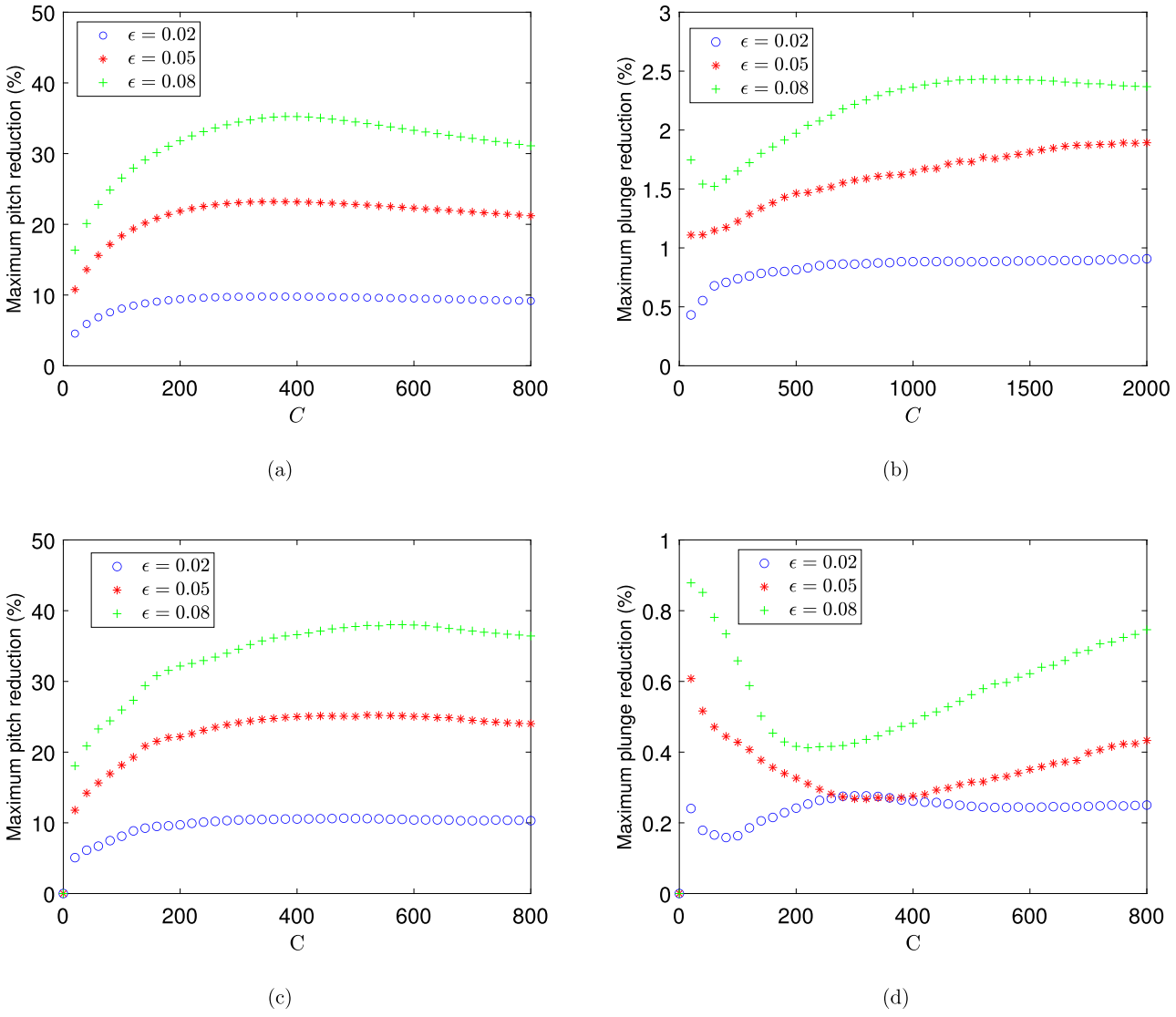

Fig. 10. The effect of NES stiffness on the gust response of the wing for $w_0 = 0.2$ a,b) sharp-edged gust profile and c,d) 1-cosine gust profile.

where $H(\tau)$ is the Heaviside step function, τ_g is half of the gust loading time, and $\bar{w}_0 = w_0/U$ is the nondimensional gust amplitude.

Following the procedure suggested in [3], the coupled aeroelastic equations (Eqs. (5)-(7)) are converted into state-space to form 12 first-order differential equations. To do this, the following new variables are introduced to deal with the integral terms in the gust and aerodynamic equations

$$w_1 = \int_0^\tau e^{-b_1(\tau-\sigma)}\alpha(\sigma)d\sigma, \qquad w_2 = \int_0^\tau e^{-b_2(\tau-\sigma)}\alpha(\sigma)d\sigma$$
$$w_3 = \int_0^\tau e^{-b_1(\tau-\sigma)}\zeta(\sigma)d\sigma, \qquad w_4 = \int_0^\tau e^{-b_2(\tau-\sigma)}\zeta(\sigma)d\sigma \tag{16}$$
$$w_5 = \int_0^\tau e^{-b_3(\tau-\sigma)}\bar{w}d\sigma, \qquad w_6 = \int_0^\tau e^{-b_4(\tau-\sigma)}\bar{w}d\sigma$$

By substituting the above variables into the equations of motion, the final nondimensional equations of motion can be obtained

$$c_0\xi'' + c_1\alpha'' + c_2\xi' + c_3\alpha' + c_4\nu' + c_5\xi + c_6\alpha + c_7w_1 + c_8w_2 + c_9w_3 + c_{10}w_4 + c_{11}w_5 + c_{12}w_6 + (\bar{\omega}/\bar{U})^2G(\zeta) + \frac{\epsilon C}{\bar{U}^2}H(\zeta,\alpha,\nu) = f(\tau) \tag{17}$$

$$d_0\xi'' + d_1\alpha'' + d_2\xi' + d_3\alpha' + d_4\nu' + d_5\xi + d_6\alpha + d_7w_1 + d_8w_2 + d_9w_3 + d_{10}w_4 + d_{11}w_5 + d_{12}w_6 + (1/\bar{U})^2M(\alpha) + \frac{\delta\epsilon C}{r_\alpha^2\bar{U}^2}N(\zeta,\alpha,\nu) = g(\tau) \tag{18}$$

$$e_0\nu'' + e_1\xi' + e_2\alpha' + e_3\nu' + \frac{C}{\bar{U}^2}P(\zeta,\alpha,\nu) = 0 \tag{19}$$

where G, H, M, N and P are nonlinear functions, and are given in the Appendix alongside coefficients $c_i(i = 0, ..., 12)$, $d_i(i = 0, ..., 12)$ and $e_i(i = 0, ..., 3)$. Furthermore, $f(\tau)$ and $g(\tau)$ are aerodynamic terms which are functions of initial conditions

$$f(\tau) = \frac{2}{\mu}[\xi(0) + (0.5 - a_h)\alpha(0)](A_1b_1e^{-b_1\tau} + A_2b_2e^{-b_2\tau}) \tag{20}$$

$$g(\tau) = -\frac{1 + 2a_h}{r_\alpha^2\mu}[\xi(0) + (0.5 - a_h)\alpha(0)](A_1b_1e^{-b_1\tau} + A_2b_2e^{-b_2\tau}) \tag{21}$$

By introducing the state vector $\boldsymbol{X} = (x_1, ..., x_{12})^T$, where

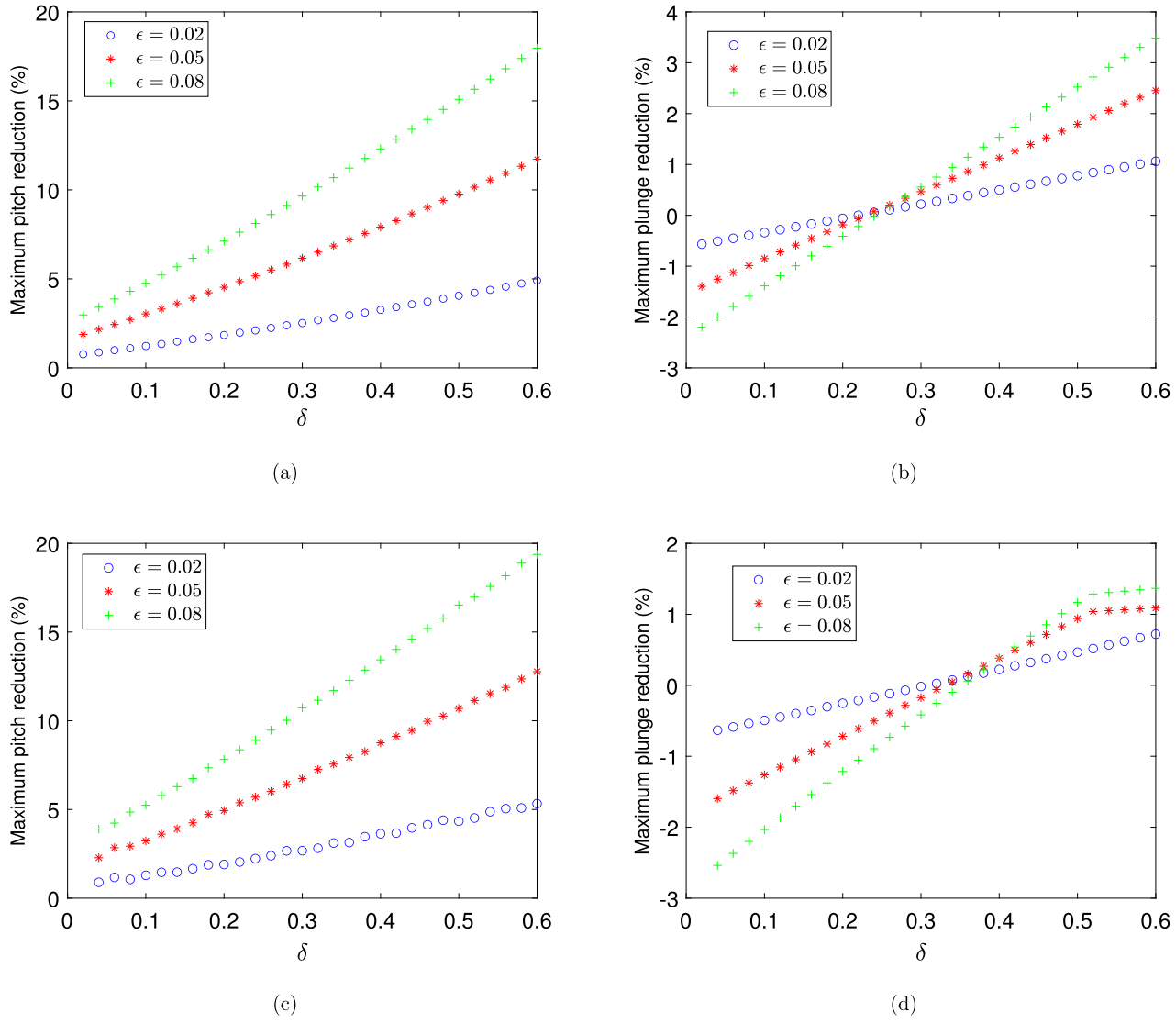

Fig. 11. The effect of NES location on the gust response of the wing for $w_0 = 0.2$ a,b) sharp-edged gust profile and c,d) 1-cosine gust profile.

$$\boldsymbol{X} = (x_1, ..., x_{12})^T = (\alpha, \alpha', \xi, \xi', \nu, \nu', w_1, w_2, w_3, w_4, w_5, w_6)^T$$

the final state-space form of the equations can be written as

$$\boldsymbol{X}' = \boldsymbol{F}(\boldsymbol{X}, \tau) \tag{22}$$

This equation is integrated numerically using an explicit Runge-Kutta (4,5) formulation [40] to find the aeroelastic time response of the wing.

3. Numerical results

3.1. Model verification

In order to check the accuracy of the developed aeroelastic model, three case studies are considered. In the first case, to check the aeroelastic response of the wing (in the absence of gust and NES), the post-instability pitch amplitude of a wing with a nonlinear spring in pitch is determined and compared with those obtained numerically by [3] in Fig. 2 and an excellent agreement is observed. In this case, a cubic hardening stiffness is assumed for the pitch degree of freedom given by

$$M(\alpha) = \beta_0 \alpha + \beta_\alpha \alpha^3 \tag{23}$$

In the second case, to evaluate the effect of the NES on the aeroelastic response of the wing, the pitch and NES amplitudes of the nonlinear wing are determined, and shown in Fig. 3. The results are in very good agreement revealing that the developed model can capture the effects of the NES on the aeroelastic response of the wing accurately. For this case, a pentic hardening nonlinearity in the pitch degree of freedom is considered such that

$$M(\alpha) = \beta_0 \alpha + \beta_\alpha \alpha^3 + \gamma_\alpha \alpha^5 \tag{24}$$

Finally, in the third case, the effect of gust loads on the pitch response for a wing with free-play nonlinearity (in the absence of NES) is obtained, and shown in Fig. 4. This comparison shows an excellent agreement between the results for both sharp-edged and 1-cosine gust profiles. Here, the following free-play nonlinearity in the pitch degree of freedom is considered [39]

$$\begin{aligned} M(\alpha) &= \alpha + 1 \quad \text{for} \quad \alpha < -1 \ \text{(deg)} \\ M(\alpha) &= 0 \quad \text{for} \quad -1 \le \alpha \le 1 \ \text{(deg)} \\ M(\alpha) &= \alpha - 1 \quad \text{for} \quad \alpha > 1 \ \text{(deg)} \end{aligned} \tag{25}$$

It can be concluded from the above three case studies, that the developed model can capture the aeroelastic and gust response of a nonlinear

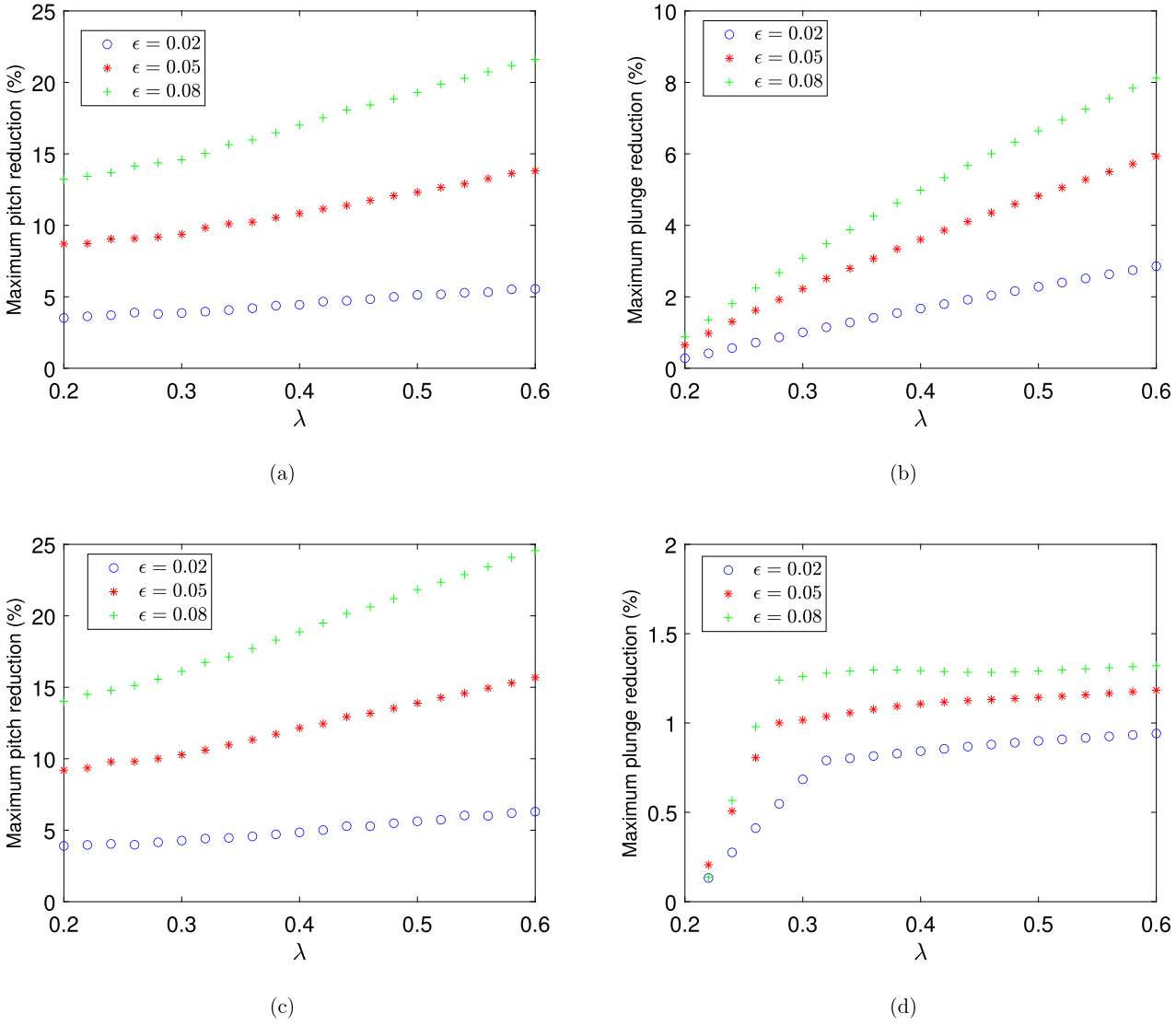

Fig. 12. The effect of NES damper on the gust response of the wing for $\omega_0 = 0.2$ a,b) sharp-edged gust profile and c,d) 1-cosine gust profile.

Table 1
The properties of the wing.

Parameter	a	μ	x_α	r_α	$\bar{\omega}$
Value	-0.5	100	0.25	0.5	0.2

Table 2
Nonlinear case studies.

Parameter	β_0	β_α
Case 1	1	40
Case 2	0.2	40

wing with the NES device accurately. In what follows, the effects of the nonlinear energy sink on the aeroelastic and gust responses of the wing are investigated.

3.2. Aeroelastic behaviour of the wing with NES

In this section, the aeroelastic behaviour of the wing with and without a nonlinear energy sink is investigated. Since the main purpose of this paper is to evaluate the effectiveness of the NES in the pre-flutter region of the wing, only one nonlinear wing case has been considered. Also, since the post-instability region of the wing in gust condition is not of high interest, the results for this part are also limited. Therefore, from here on, a wing with the properties presented in Table 1 with cubic nonlinearity as presented in Eq. (23) is considered, and all the initial conditions are considered to be zero except the initial pitch which is $\alpha(0) = 0.1^o$.

It is noted that the linear nondimensional flutter speed of this wing for $\beta_0 = 1$ and $\beta_\alpha = 0$ is obtained as $\bar{U}_f = 6.285$ which is similar to the one reported by Lee et al. [3]. To evaluate the effect of the NES parameters on the pre and post flutter behaviour of the wing, two case studies, as presented in Table 2, are considered. It is noted that the only difference between these two cases is the stiffness of the linear spring which results in different onsets of instability speeds. Fig. 5 shows the effect of NES mass ratio on the pitch and NES responses. It is noted that here that a baseline NES with values presented in Table 3 is considered. The addition of the NES has minor effects on the onset of flutter instability (also reported by [15]), but it affects the post flutter behaviour of the wing. Above the instability speed, the NES initially is not help-

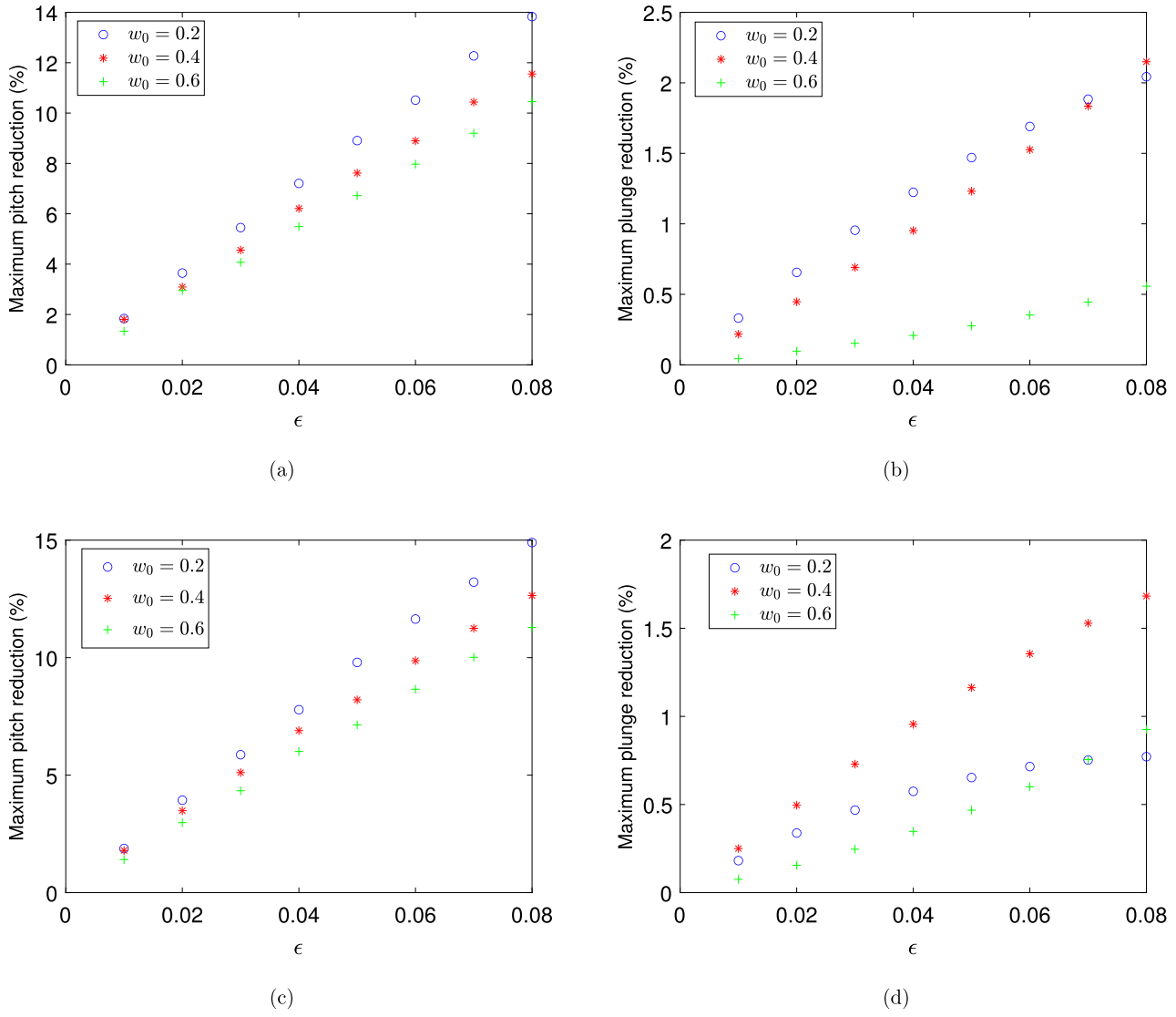

Fig. 13. The effect of gust amplitude and NES mass ratio on the gust response of the wing for $\tau_g = 800$ a,b) sharp-edged gust profile and c,d) 1-cosine gust profile.

Table 3
The nonlinear energy sink baseline values.

Parameter	C	λ	ϵ	δ
Value	10	0.25	0.01	0.45

ful in reducing the oscillation amplitude, and even increases it slightly. However, when the wing oscillation amplitude increases, then the NES starts to be effective which can be seen as a jump in the NES bifurcation plots. It is noted that the speed at which this jump happens is strictly dependent on the NES mass ratio (ϵ). As the mass ratio increases, the jump speed increases. At the same time, as the mass ratio increases, the amplitude reduction magnitude increases.

Fig. 6 shows the bifurcation diagrams for the case 2 wing. It is noted that due to the weaker linear spring stiffness for this case, the onset of instability is less than the flutter speed of case 1. In this case, the wing undergoes various motions (period-1, period-1-h, period-3, chaotic), and adding the NES changes the speed at which the oscillation period changes. Furthermore, by increasing the mass ratio, the speed at which the period switching happens increases. It is noted that as the level of NES displacement is high, this could be an important limitation of this concept in real application, and hence other more compact NES concepts such as vibro-impact NES or rotational NES will be studied in the future to overcome this limitation.

Next, the effect of NES stiffness on the aeroelastic response of both wings is investigated and shown in Fig. 7 (only for the upper branch of co-existing solutions). For case 1 and for all mass ratios, by increasing the NES stiffness, the pitch response amplitude first increases, then decreases and again slightly increases. While, for case 2, the situation is different as the response is different between various mass ratios. For smaller mass ratios, by increasing the NES stiffness, the pitch response first increases and then decreases gradually. However, for larger mass ratios, the response first decreases, then increases and finally gradually decreases again. It is noted that the stiffness values at which these changes happen are different for various mass ratios. This behaviour highlights that the NES stiffness needs to be optimised for each specific system.

Fig. 8 shows the effect of NES offset from the wing elastic axis on the upper branch of co-existing solutions of pitch response for both wings. As the NES moves away from the elastic axis, the pitch amplitude changes for both cases. In case 1 and for small values of mass ratio, by moving the NES toward tip, the pitch amplitude gradually decreases. However, for larger mass ratios, the pitch amplitude first decreases until

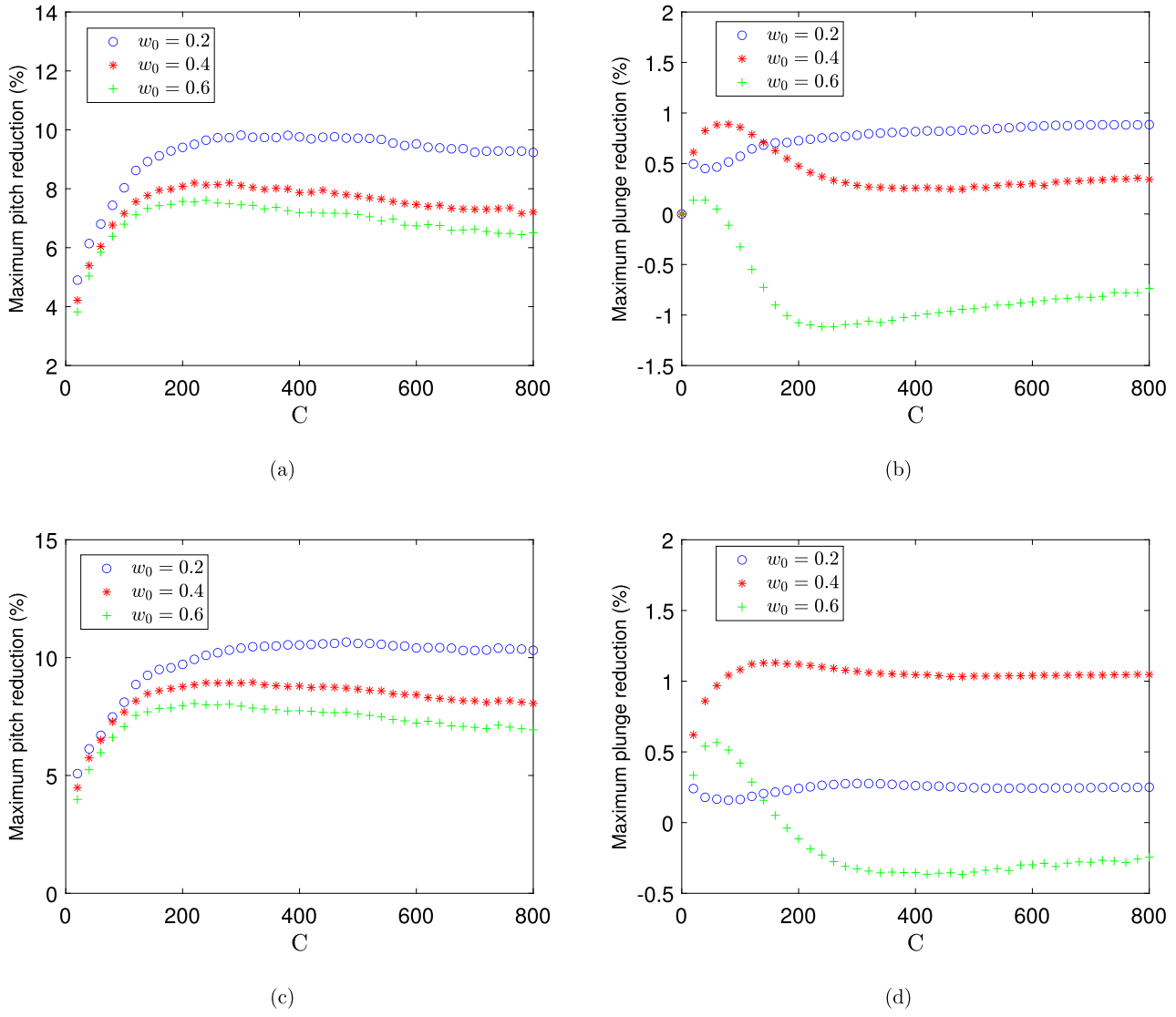

Fig. 14. The effect of gust amplitude and NES stiffness on the gust response of the wing for $\tau_g = 800$ a,b) sharp-edged gust profile and c,d) 1-cosine gust profile.

a point at which the pitch amplitude suddenly jumps up. And then from this point onward, the amplitude again decreases. Therefore, depending on the value of the mass ratio, there could be one specific location that can result in the highest amplitude reduction of the wing. A similar trend is observed for case 2, but in this case the sudden jump seen in case 1 doesn't exist any more.

3.3. Gust response of the wing with NES

In the previous section, the effect of adding an NES to the wing on the aeroelastic response of the wing in the post-instability region has been studied. In this section, the capability of the NES on gust load/response reduction of the wing is investigated. It is noted that here, unless otherwise stated, the baseline NES values are considered for all parametric studies. As mentioned before, two gust profiles are considered which are the sharp-edged and 1-cosine gust profiles. It is noted that in this section, only the case 1 wing will be considered, but similar conclusions may be obtained for wing 2 as well.

First, it is assumed that the aircraft is flying in the stable region ($\bar{U}/\bar{U}_f = 0.8$) at which the gust hits the wing. Fig. 9 shows the effect of the NES mass ratio on the gust response of the wing for both gust profiles. This clearly shows that when the NES is added to the wing, it has the potential to reduce the maximum response amplitude of the wing. However, in this case the maximum amplitude reduction is very small, but this is due to the fact that the NES parameters are not optimum. This means that adding an NES can be helpful to attenuate the gust loads on the wing. In this case, as the NES mass ratio increases, the maximum amplitude reduction increases for both gust profiles.

Fig. 10 shows the effect of NES spring stiffness on the maximum pitch amplitude reduction of the wing for both gust profiles. For both profiles, as the stiffness value increases, the maximum pitch amplitude reduction increases, and then remains almost the same or decreases slightly, depending on the value of mass ratio. This behaviour means that there is a specific value of stiffness that can result in the highest pitch amplitude reduction for the wing. It is noted that this optimum value is dependent to the mass ratio of the NES and airflow velocity. Furthermore, it can be seen that the NES is more effective for the sharp-edged gust load reduction than the 1-cosine gust load reduction Moreover, the plunge amplitude reduction does not follow the same trend as the pitch amplitude reduction for high mass ratios. For higher mass ratios, the plunge amplitude reduction first decreases and then increases. It is noted that the NES is more effective in pitch amplitude reduction.

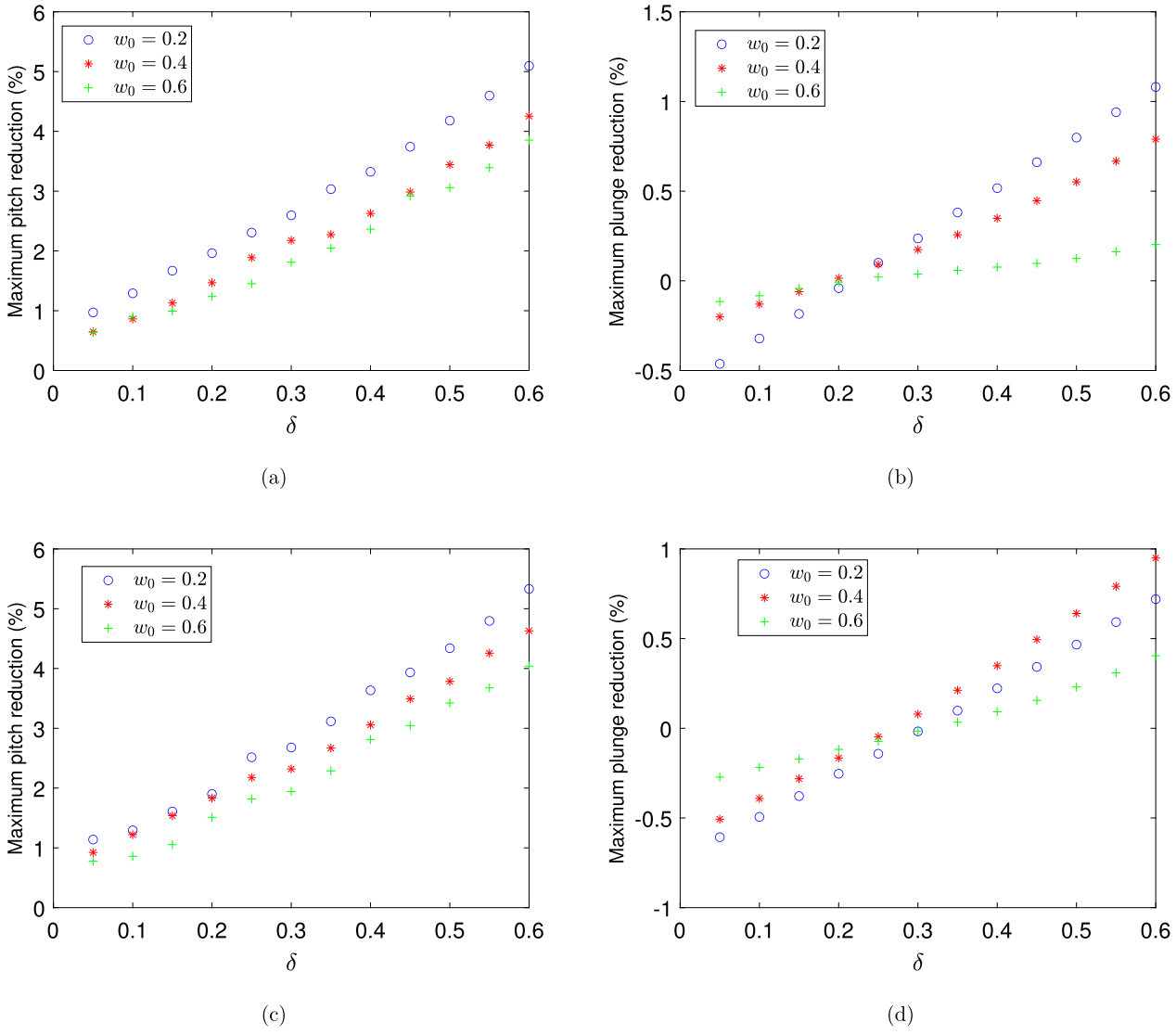

Fig. 15. The effect of gust amplitude and NES location on the gust response of the wing for $\tau_g = 800$ a,b) sharp-edged gust profile and c,d) 1-cosine gust profile.

The effect of NES location on the gust response of the wing is determined next and shown in Fig. 11. By moving the NES towards the wing tip, the gust response amplitude gradually decreases for both gust profiles. As for the previous cases, as the mass ratio increases, the amount of gust load reduction increases. It is noted that there is a specific NES location at which the NES becomes effective for plunge amplitude reduction. This location is dependent on the gust profile. Moreover, the effect of the NES linear damper on the gust response reduction of the wing is shown in Fig. 12. As the damper value increases, the maximum gust amplitude reduces for all cases. But, the rate of change is not uniform between pitch and plunge responses.

Next, the effect of gust amplitude on the NES effectiveness has been considered. Figs. 13–16 show the maximum gust response amplitude reduction for various NES parameters. The effect of NES mass ratio and gust amplitude on the wing pitch and plunge gust response is shown in Fig. 13. By increasing the NES mass ratio, the maximum gust response amplitude reduces for all gust amplitudes. However, for higher gust amplitudes, the NES is less capable in reducing the gust load. But, this is not true for the plunge response of the 1-cosine gust case. Fig. 14 shows the effect of NES stiffness on wing gust response reduction for various gust amplitudes. For this case, again the capability of the NES reduces as the gust amplitude increases. Furthermore, the stiffness at which the gust load reduction trend switches from increase to decrease is different for each gust amplitude. Figs. 15 and 16 show again the same trend for the NES gust response reduction effectiveness for different gust amplitudes. Fig. 17 shows the effectiveness of the NES for pitch response reduction of the wing for various values of gust loading time for a 1-cosine gust profile. As the gust loading time increases, the NES becomes slightly more effective. It is noted that the stiffness value at which the highest load reduction happens is completely different for various gust loading times. So, this reveals that there is no optimum NES value which can be used for all gust conditions, and hence, a tunable NES with various stiffness or mass is desired. This can be considered in future studies.

By considering the near optimum values of NES for pitch amplitude reduction (shown in the previous parametric studies) and for one gust condition ($\omega_0 = 0.2, \tau_g = 800$), Fig. 18 shows the gust response of the wing with and without the optimum NES. In this case at an airflow velocity of $\bar{U}/\bar{U}_f = 0.8$, the NES is able to reduce the maximum pitch amplitude by up to 43% and 41% for sharp-edged and 1-cosine gust profiles, respectively. This highlights the potential effectiveness of the NES in reducing the response amplitude and hence load reduction. Furthermore, to investigate the displacement of the NES, the relative

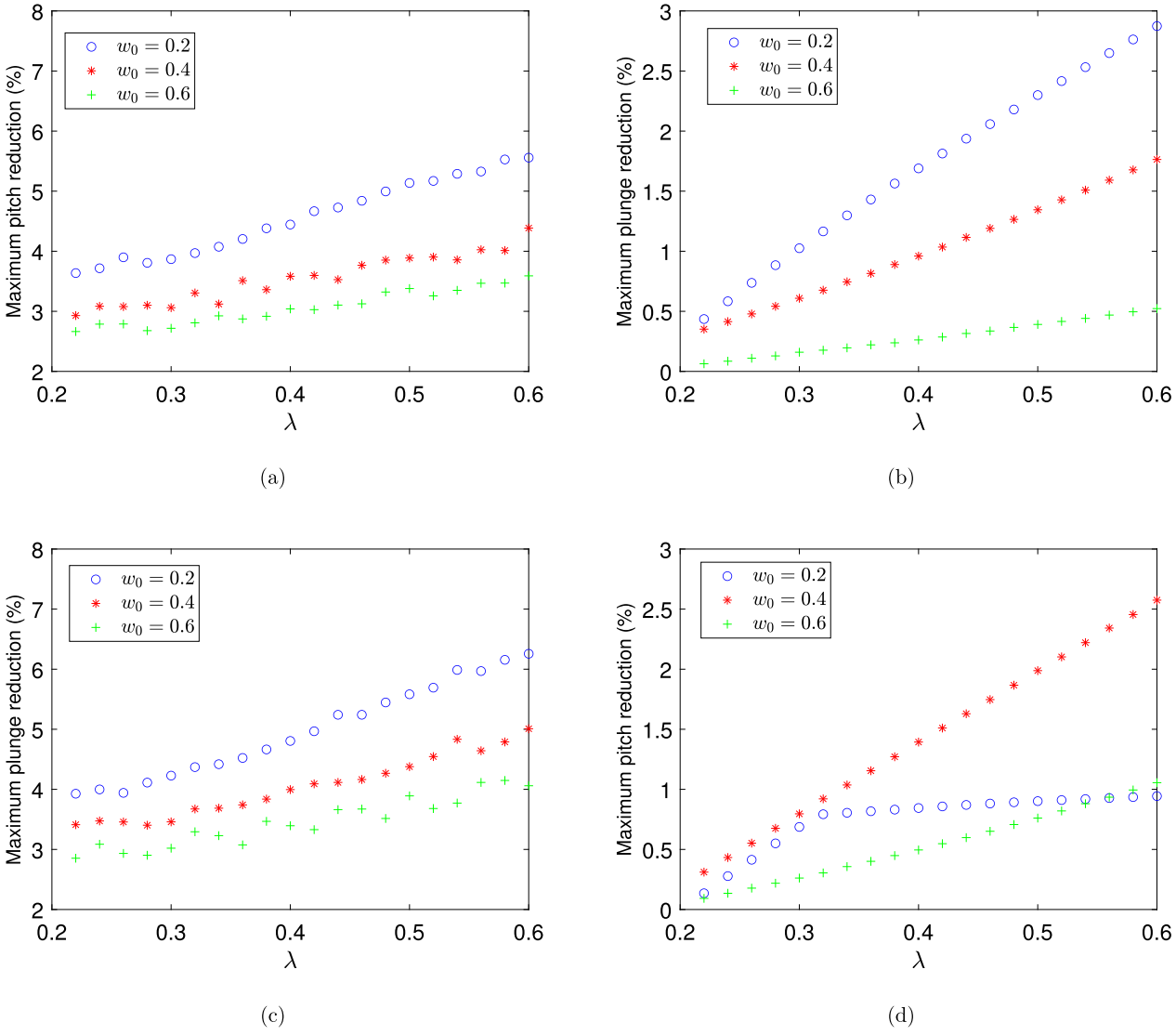

Fig. 16. The effect of gust amplitude and NES damper on the gust response of the wing for $\tau_g = 800$ a,b) sharp-edged gust profile and c,d) 1-cosine gust profile.

nondimensional displacement of the NES with respect to the wing for these two optimum cases are determined and shown in Fig. 19.

Finally, the effect of the optimum NES on the gust response of the wing in the post-instability region for various speeds are investigated. Figs. 20–22 show the aeroelastic response of the wing with and without gusts and NES. In this case, the NES is still capable of reducing the pitch amplitude of the wing, and its effectiveness. Also, the gust load reduction due to NES increases as the post-instability speed increases. This highlights the effectiveness of adding an NES to the wing to reduce the gust loads in both pre and post instability regions.

4. Conclusion

In this paper, the effectiveness of a nonlinear energy sink on the aeroelastic and gust response of a wing was investigated. The structural dynamics of the wing was simulated using a two dimensional airfoil which has a hardening nonlinearity in the pitch degree of freedom. Also, the aerodynamic loads applied on the wing were modelled using Wagner's unsteady lifting line theory. The wing was assumed to be subjected to gust loads which are simulated using two gust profiles which are sharp-edged and 1-cosine profiles. A nonlinear energy sink was attached to the wing with an offset from the wing elastic axis. The dynamics of the NES was simulated using a concentrated mass connected to the wing through a linear damper and a nonlinear spring. The final aeroelastic differential equations were transferred to state-space form, and solved using numerical integration. To check the accuracy of the developed aeroelastic model, various case studies were considered and the results were compared with those available in the literature and an excellent agreement was observed. Then, the effect of various wing and NES parameters on the aeroelastic and gust response of the wing were investigated. It was found that adding a nonlinear energy sink to the wing has the capability of reducing the aeroelastic and gust response amplitudes, for both pre and post-instability regions, and hence can reduce the loads. Furthermore, it was observed that the NES can also affect the periodic behaviour of the wing in the post-flutter region. Finally, it was highlighted that if the NES parameters are selected properly, it is possible to reduce the gust response amplitude depending on the gust condition. However, it is more desirable to design a tunable NES which can reduce the gust amplitude for different gust conditions. Future work will include designing a tunable NES and its application to a 3D wing model.

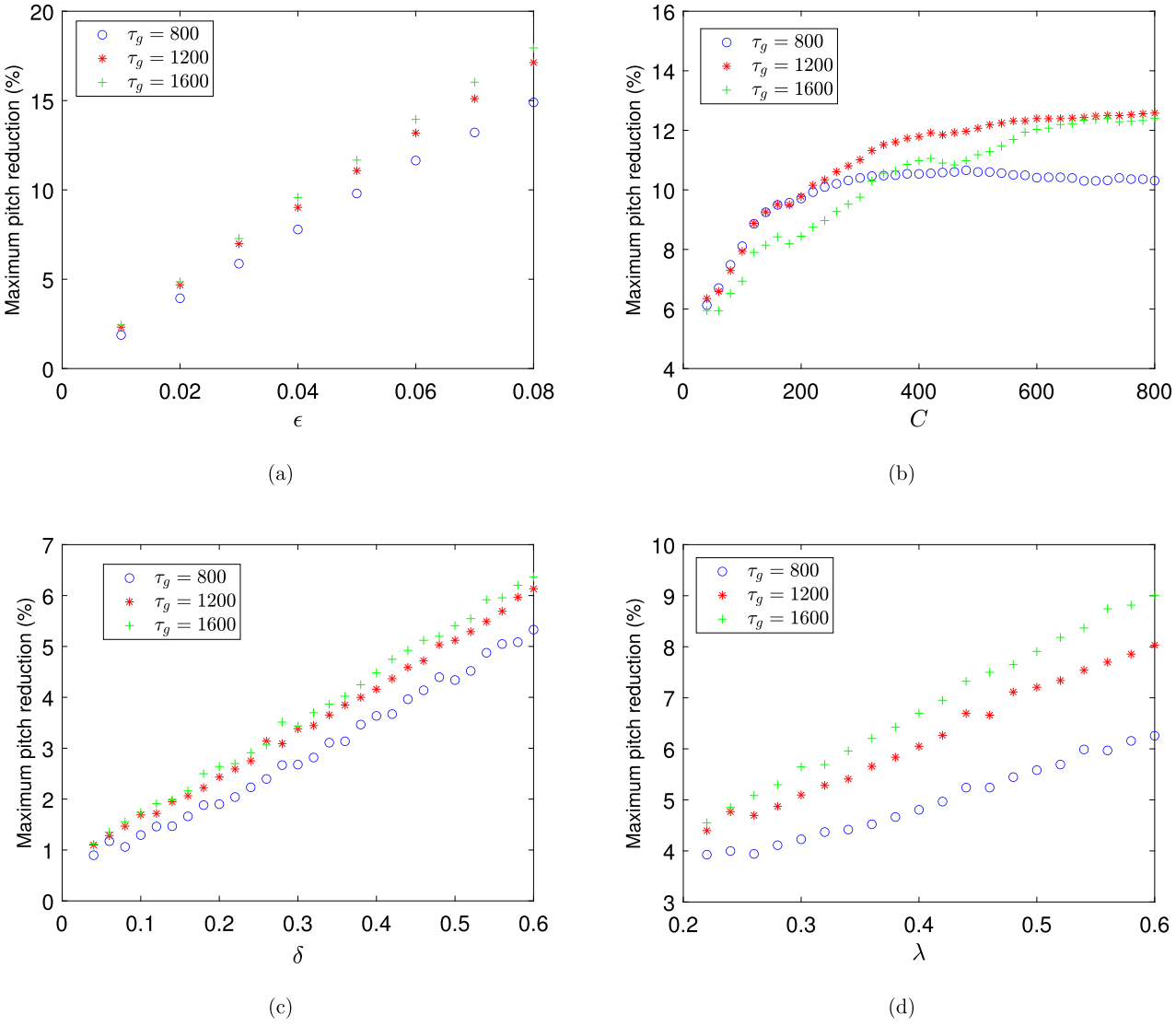

Fig. 17. The effect of gust loading time on the 1-cosine gust response of the wing for $w_0 = 0.2$, and for various values of a) NES mass ratio, b) NES stiffness, c)NES location and d) NES damper.

CRediT authorship contribution statement

M.R. Amoozgar: Conceptualization, Data curation, Formal analysis, Investigation, Methodology, Software, Validation, Visualization, Writing – original draft, Writing – review & editing. **A. Castrichini:** Writing – review & editing. **S.D. Garvey:** Writing – review & editing. **M.I. Friswell:** Writing – review & editing. **J.E. Cooper:** Writing – review & editing. **R.M. Ajaj:** Writing – review & editing.

Declaration of competing interest

The authors declare that they have no known competing financial interests or personal relationships that could have appeared to influence the work reported in this paper.

Data availability

Data will be made available on request.

Appendix A. Coefficients in Eq. (17)-(19)

$$c_0 = 1 + \frac{1}{\mu}, c_1 = x_\alpha - \frac{a_h}{\mu}, c_2 = 2\zeta_\xi \frac{\bar{\omega}}{\bar{u}} + \frac{2}{\mu}(1 - A_1 - A_2) + \frac{\epsilon\lambda}{\bar{U}},$$

$$c_3 = \frac{2}{\mu}(1 + (1 - 2a_h)(1 - A_1 - A_2)) - \frac{\epsilon\lambda\delta}{\bar{U}}, c_4 = -\frac{\epsilon\lambda}{\bar{U}},$$

$$c_5 = \frac{2}{\mu}(b_1 A_1 + b_2 A_2)$$

$$c_6 = \frac{2}{\mu}(1 - A_1 - A_2 + (0.5 - a_h)(b_1 A_1 + b_2 A_2)),$$

$$c_7 = \frac{2}{\mu} b_1 A_1 (1 - b_1(0.5 - a_h)), c_8 = \frac{2}{\mu} b_2 A_2 (1 - b_2(0.5 - a_h)),$$

$$c_9 = -\frac{2}{\mu} b_1^2 A_1, c_{10} = -\frac{2}{\mu} b_2^2 A_2, c_{11} = -\frac{2}{\mu} b_3 A_3, c_{12} = -\frac{2}{\mu} b_4 A_4$$

$$d_0 = \frac{x_\alpha}{r_\alpha^2} - \frac{a_h}{\mu r_\alpha^2}, d_1 = 1 + \frac{1 + 8a_h^2}{8\mu r_\alpha^2},$$

$$d_2 = -\frac{1 + 2a_h}{\mu r_\alpha^2}(1 - A_1 - A_2) - \frac{\epsilon\lambda\delta}{r_\alpha^2 \bar{U}},$$

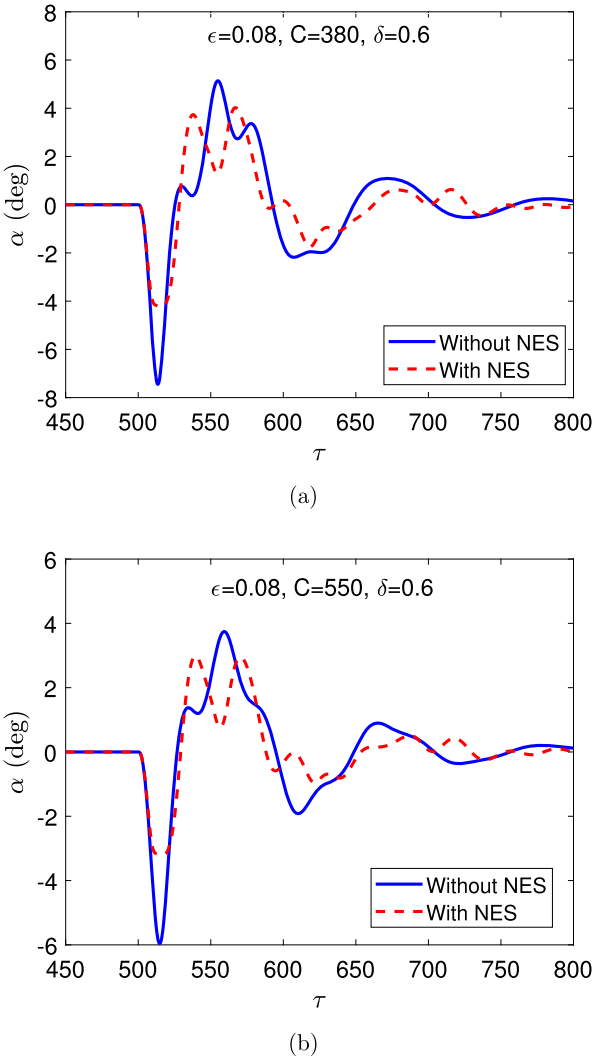

Fig. 18. The effect of the optimum NES on the gust response of the wing a) sharp-edged gust profile and b) 1-cosine gust profile.

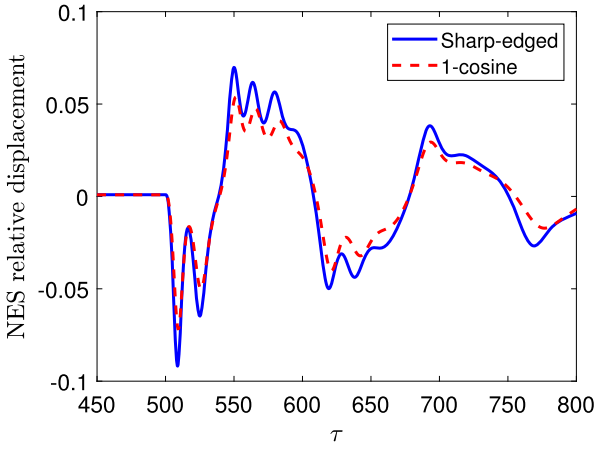

Fig. 19. The relative displacement of the NES for the optimum cases.

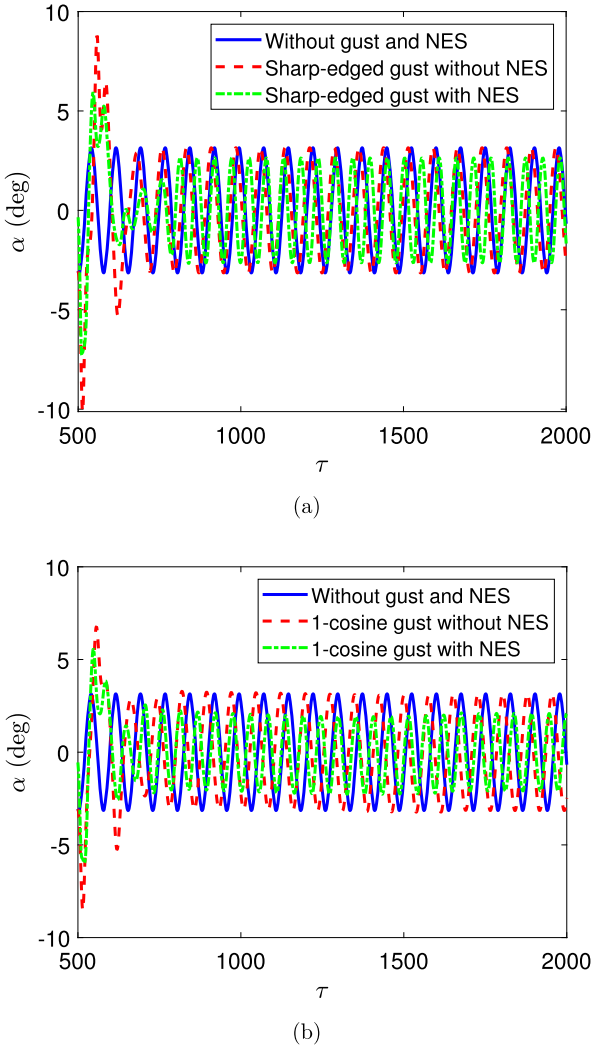

Fig. 20. The effect of the optimum NES on the gust response of the wing in the post-instability region at $\bar{U}/\bar{U}_f = 1.05$ a) sharp-edged gust profile b) 1-cosine gust profile.

$$d_3 = \frac{1-2a_h}{2\mu r_\alpha^2} - \frac{(1+2a_h)(1-2a_h)(1-A_1-A_2)}{2\mu r_\alpha^2} + \frac{\epsilon\lambda\delta^2}{r_\alpha^2\bar{U}},$$

$$d_4 = \frac{\epsilon\lambda\delta}{r_\alpha^2\bar{U}}, d_5 = -\frac{1+2a_h}{\mu r_\alpha^2}(b_1A_1 + b_2A_2),$$

$$d_6 = -\frac{1+2a_h}{\mu r_\alpha^2}(1-b_1-b_2) - \frac{(1+2a_h)(1-2a_h)(A_1b_1 - A_2b_2)}{2\mu r_\alpha^2},$$

$$d_7 = -\frac{(1+2a_h)A_1b_1}{\mu r_\alpha^2}(1-b_1(0.5-a_h)),$$

$$d_8 = -\frac{(1+2a_h)A_2b_2}{\mu r_\alpha^2}(1-b_2(0.5-a_h)),$$

$$d_9 = \frac{(1+2a_h)b_1A_1^2}{\mu r_\alpha^2}, d_{10} = \frac{(1+2a_h)b_2A_2^2}{\mu r_\alpha^2},$$

$$d_{11} = -\frac{2}{\mu r_\alpha^2}(0.5+a_h)A_3b_3, d_{12} = -\frac{2}{\mu r_\alpha^2}(0.5+a_h)A_4b_4,$$

$$e_0 = 1, e_1 = -\frac{\lambda}{\bar{U}}, e_2 = \frac{\lambda\delta}{\bar{U}}, e_3 = \frac{\lambda}{\bar{U}}$$

$$H = (\xi - \delta\alpha - \nu)^3, N = (\delta\alpha + \nu - \xi)^3, P = (\delta\alpha + \nu - \xi)^3.$$

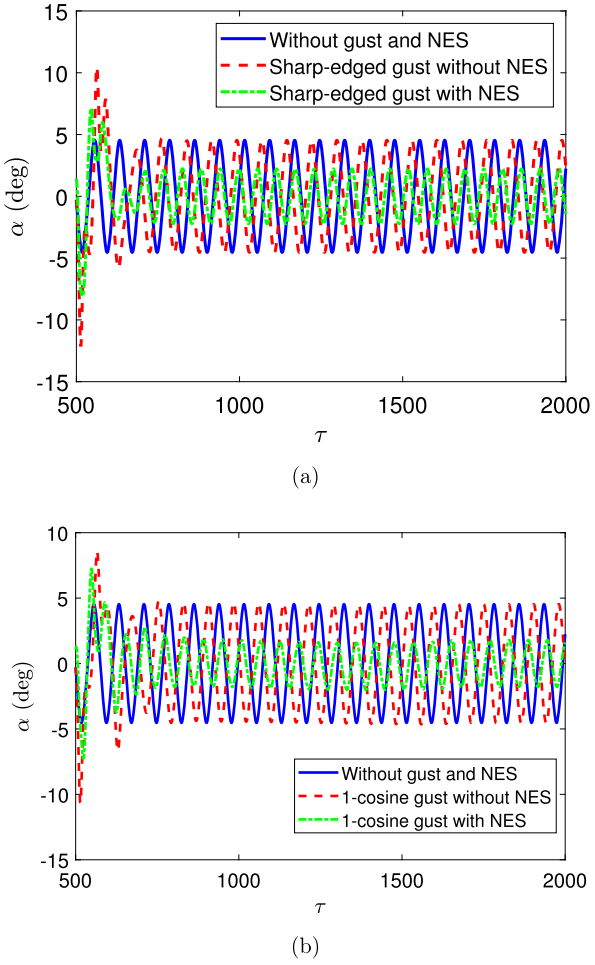

Fig. 21. The effect of the optimum NES on the gust response of the wing in the post-instability region at $\bar{U}/\bar{U}_f = 1.10$ a) sharp-edged gust profile b) 1-cosine gust profile.

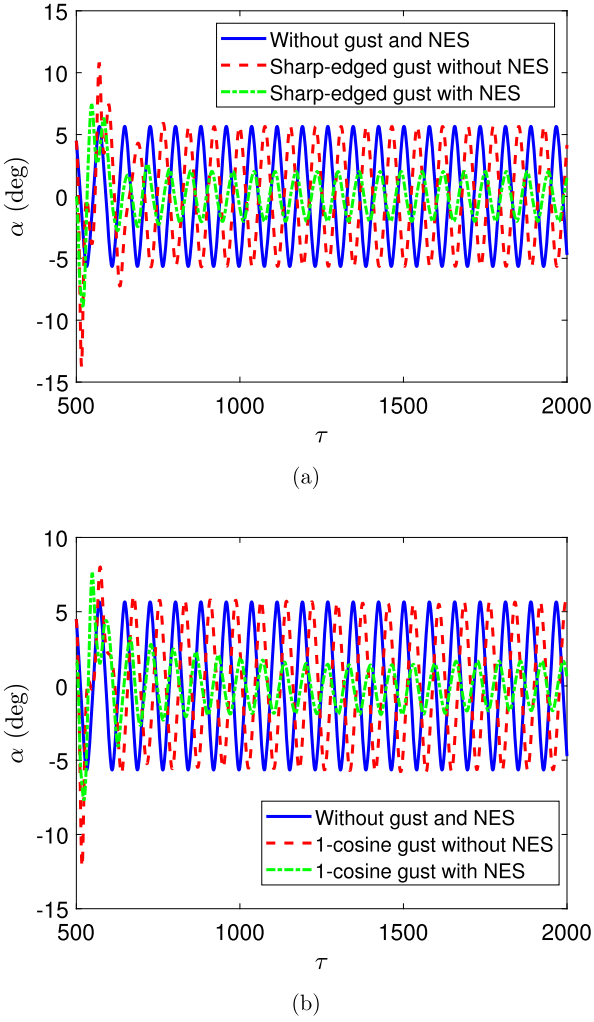

Fig. 22. The effect of the optimum NES on the gust response of the wing in the post-instability region at $\bar{U}/\bar{U}_f = 1.15$ a) sharp-edged gust profile b) 1-cosine gust profile.

References

[1] Raymond L. Bisplinghoff, Holt Ashley, Principles of Aeroelasticity, Wiley & Sons, New York, 1962.

[2] Jan R. Wright, Jonathan E. Cooper, Introduction to Aircraft Aeroelasticity and Loads, Wiley & Sons, New York, 2014.

[3] B.H.K. Lee, S.J. Price, Y.S. Wong, Nonlinear aeroelastic analysis of airfoils: bifurcation and chaos, Prog. Aerosp. Sci. 35 (3) (1999) 205–334.

[4] Elmar J. Breitbach, Flutter analysis of an airplane with multiple structural nonlinearities in the control system, NACA TP-1620. 1980.

[5] Hui Zhang, Zhi-Chun Yang, Xin-Ping Zhang, Jian Zhou, Ying-Song Gu, Effects of structural parameters on chaotic motion behavior of nonlinear flutter for a two dimensional wing, Zhendong yu Chongji (Journal of Vibration and Shock) 32 (12) (2013).

[6] Xiaoyang Zhang, Mojtaba Kheiri, Wen-Fang Xie, Aeroservoelasticity of an airfoil with parametric uncertainty and subjected to atmospheric gusts, AIAA J. 59 (11) (2021).

[7] Saied Irani, Hamid Sarrafzadeh, Mohammad Reza Amoozgar, Bifurcation in a 3-dof airfoil with cubic structural nonlinearity, Chin. J. Aeronaut. 24 (3) (2011) 265–278.

[8] Donald S. Woolston, Harry L. Runyan, Robert E. Andrews, An investigation of effects of certain types of structural nonlinearities on wing and control surface flutter, J. Aeronaut. Sci. 24 (1) (1957) 57–63.

[9] B.H.K. Lee, J. Desrochers, Flutter Analysis of a Two-Dimensional Airfoil Containing Structural Nonlinearities, National Aeronautical Establishment, Ottawa, Ontario, 1987.

[10] Xing Li, Yuguang Bai, Ling Xiao, Wei Qian, Junning Su, Vibration control studies of a high-aspect-ratio wing with geometric nonlinearity, Aerosp. Sci. Technol. 123 (2022) 107461.

[11] Leonardo Sanches, Thiago A.M. Guimarães, Flávio D. Marques, Aeroelastic tailoring of nonlinear typical section using the method of multiple scales to predict post-flutter stable lcos, Aerosp. Sci. Technol. 90 (2019) 157–168.

[12] Martin Sohst, José Lobo do Vale, Frederico Afonso, Afzal Suleman, Optimization and comparison of strut-braced and high aspect ratio wing aircraft configurations including flutter analysis with geometric non-linearities, Aerosp. Sci. Technol. 124 (2022) 107531.

[13] Ying Hao, Chao Ma, Yuda Hu, Nonlinear stochastic flutter analysis of a three-degree-of-freedom wing in a two-dimensional flow field under stochastic perturbations, Aerosp. Sci. Technol. 138 (2023) 108323.

[14] Bharath Pidaparthi, Samy Missoum, Stochastic optimization of nonlinear energy sinks for the mitigation of limit cycle oscillations, AIAA J. 57 (5) (2019) 2134–2144.

[15] Youssef Bichiou, Muhammad R. Hajj, Ali H. Nayfeh, Effectiveness of a nonlinear energy sink in the control of an aeroelastic system, Nonlinear Dyn. 86 (4) (2016) 2161–2177.

[16] Ira P. Wall, Mohammadreza Amoozgar, Atanas Popov, Vibration attenuation of rotating blades using a non-linear energy sink, in: AIAA AVIATION 2023 Forum, 2023, https://doi.org/10.2514/6.2023-3952.

[17] A.F. Vakakis, O.V. Gendelman, L.A. Bergman, D.M. McFarland, G. Kerschen, Y.S. Lee, Nonlinear Targeted Energy Transfer in Mechanical and Structural Systems, Springer, 2008.

[18] Xiaoai Jiang, D. Michael McFarland, Lawrence A. Bergman, Alexander F. Vakakis, Steady state passive nonlinear energy pumping in coupled oscillators: theoretical and experimental results, Nonlinear Dyn. 33 (1) (2003) 87–102.

[19] Pramod Malatkar, Ali H. Nayfeh, Steady-state dynamics of a linear structure weakly coupled to an essentially nonlinear oscillator, Nonlinear Dyn. 47 (1) (2007) 167–179.

[20] Wei Tian, Yueming Li, Ping Li, Zhichun Yang, Tian Zhao, Passive control of nonlinear aeroelasticity in hypersonic 3-d wing with a nonlinear energy sink, J. Sound Vib. 462 (2019) 114942.

[21] Jian Zhou, Minglong Xu, Zhichun Yang, Yingsong Gu, Suppression of panel flutter response in supersonic airflow using a nonlinear vibration absorber, Int. J. Non-Linear Mech. 133 (2021) 103714.

[22] Christopher P. Szczyglowski, Simon A. Neild, Branislav Titurus, Jason Z. Jiang, Etienne Coetzee, Passive gust loads alleviation in a truss-braced wing using an inerter-based device, J. Aircr. 56 (6) (2019) 2260–2271.
[23] Hamed Khodaparast, Georgia Georgiou, Jonathan E. Cooper, Luigi Riccobenne, Sergio Ricci, Gareth Vio, Peter Denner, Rapid prediction of worst case gust loads, J. Aeroelast. Struct. Dyn. 2 (3) (2012) 33–54.
[24] Dominique C. Poirel, Stuart J. Price, Post-instability behavior of a structurally nonlinear airfoil in longitudinal turbulence, J. Aircr. 34 (5) (1997) 619–626.
[25] Deman Tang, Earl H. Dowell, Experimental and theoretical study of gust response for high-aspect-ratio wing, AIAA J. 40 (3) (2002) 419–429.
[26] Robbie Cook, Dario Calderon, Mark H. Lowenberg, Simon Nield, Jonathan E. Cooper, Etienne Coetzee, Worst case gust prediction of highly flexible wings, in: 58th AIAA/ASCE/AHS/ASC Structures, Structural Dynamics, and Materials Conference, Number AIAA 2017-1355, 2017.
[27] H. Haddad Khodaparast, J.E. Cooper, Rapid prediction of worst-case gust loads following structural modification, AIAA J. 52 (2) (2014) 242–254.
[28] Davide Balatti, Hamed Haddad Khodaparast, Michael I. Friswell, Marinos Manolesos, Mohammadreza Amoozgar, The effect of folding wingtips on the worst-case gust loads of a simplified aircraft model, Proc. Inst. Mech. Eng., G J. Aerosp. Eng. 236 (2) (2022) 219–237.
[29] Davide Balatti, Hamed Haddad Khodaparast, Michael I. Friswell, Marinos Manolesos, Andrea Castrichini, Aircraft turbulence and gust identification using simulated in-flight data, Aerosp. Sci. Technol. 115 (2021) 106805.
[30] Yonghong Li, Ning Qin, Gust load alleviation by normal microjet, Aerosp. Sci. Technol. 117 (2021) 106919.
[31] A. Castrichini, V. Hodigere Siddaramaiah, D.E. Calderon, J.E. Cooper, T. Wilson, Y. Lemmens, Nonlinear folding wing tips for gust loads alleviation, J. Aircr. 53 (5) (2016) 1391–1399.
[32] Bi Ying, Xie Changchuan, An Chao, Yang Chao, Gust load alleviation wind tunnel tests of a large-aspect-ratio flexible wing with piezoelectric control, Chin. J. Aeronaut. 30 (1) (2017) 292–309.
[33] A. Khalil, N. Fezans, Gust load alleviation for flexible aircraft using discrete-time, Aeronaut. J. 125 (1284) (2021) 341–364.
[34] Fintan Healy, Ronald C. Cheung, Djamel Rezgui, Jonathan E. Cooper, Thomas Wilson, Andrea Castrichini, On the nonlinear geometric behaviour of flared folding wingtips, in: AIAA SCITECH 2022 Forum, 2022.
[35] Ronald C.M. Cheung, Djamel Rezgui, Jonathan E. Cooper, Thomas Wilson, Testing of a hinged wingtip device for gust loads alleviation, J. Aircr. 55 (5) (2018) 2050–2067.
[36] Davide Balatti, Hamed Haddad Khodaparast, Michael I. Friswell, Marinos Manolesos, Andrea Castrichini, Experimental and numerical investigation of an aircraft wing with hinged wingtip for gust load alleviation, J. Fluids Struct. 119 (2023) 103892.
[37] Joe J. De Courcy, Lucian Constantin, Branislav Titurus, T. Rendall, Jonathan E. Cooper, Gust loads alleviation using sloshing fuel, in: AIAA Scitech 2021 Forum, 2021, https://doi.org/10.2514/6.2021-1152.
[38] Matthias Wuestenhagen, Gust load alleviation control of aircraft with varying mass distribution, in: AIAA SCITECH 2023 Forum, 2023, https://doi.org/10.2514/6.2023-0371.
[39] Xiaoyang Zhang, Mojtaba Kheiri, Wen-Fang Xie, Nonlinear dynamics and gust response of a two-dimensional wing, Int. J. Non-Linear Mech. 123 (2020) 103478.
[40] J.R. Dormand, P.J. Prince, A family of embedded Runge-Kutta formulae, J. Comput. Appl. Math. 6 (1) (1980) 19–26.